eration in UAS-*shi*^{ts1} photoreceptors. Rhabdomeres were largely intact, vacuolated cells were fewer, and trapezoidal arrangement of rhabdomeres was retained (Fig. 2B). As in other degenerating mutants, rhodopsin levels were low in *shi*^{ts1} mutants compared with those of the wild type but were restored upon ceramidase expression (Fig. 2C).

We then investigated whether SPT, the rate-limiting enzyme of the de novo sphingolipid biosynthetic pathway, could affect the degeneration observed in these mutants. In *Drosophila*, the Lace gene encodes the LCB2 subunit of SPT. The P-*lacW*-inserted *lace* allele *l(2)k05305* is an insertion of a P-element 8 to 9 base pairs upstream of the transcription start site of *lace* and is homozygous lethal (*16*). We crossed *arr2*^{3} and UAS-*shi*^{ts1} mutants into the *lace* heterozygous background and examined photoreceptors by transmission electron microscopy. *lace* heterozygotes had intact photoreceptors (Fig. 3A). *lace* partially suppressed retinal degeneration in *arr2*^{3} mutants (compare Fig. 3, B and C) and in UAS-*shi*^{ts1} mutants (compare Fig. 3, D and E).

Finally, we examined whether ceramidase and *lace* suppressed degeneration in a phospholipase C mutant, where endocytosis has been implicated in the degenerative process (*11*, *21*). *Norp A* encodes an eye-specific phospholipase C that activates GPCR signaling by generating inositol trisphosphate and diacylglycerol. *norp A* mutant flies do not show light-induced receptor potential and are blind (*22*). Although *norp A* mutants degenerated slowly, these changes were obvious even in 3-day-old flies (Fig. 3F). Expression of ceramidase in a *norp A* mutant suppressed retinal degeneration (Fig. 3G). *Lace* heterozygotes also suppressed *norp A* degeneration (Fig. 3H). *arr2*^{3} mutants undergo necrotic cell death, whereas *norp A* mutants accumulate rhodopsin-arrestin complexes and undergo apoptotic cell death (*10*, *11*). Thus, regardless of the mode of cell death ceramidase expression and *lace* mutant rescued degeneration. Because they also suppressed degeneration in a dynamin mutant, we infer that the sphingolipid pathway exerts its beneficial effect by altering the dynamics of the endocytic process. This is supported by observations that a sphingoid base is required for yeast endocytosis and that in mammalian cells ceramide analogs modulate fluid-phase and receptor-mediated endocytosis (*4*). The molecular details of suppression of retinal degeneration by ceramidase overexpression and *lace* mutant remain to be elucidated. A common denominator in both situations is the likely decrease in concentrations of ceramide, which could be responsible for activating a cascade that suppresses degeneration.

A large volume of work suggests that receptor desensitization, endocytosis, and recycling play a crucial role in GPCR signaling in higher organisms (*23*). In light of our finding, it will be interesting to study sphingolipid metabolism in GPCR-mediated processes. Several inherited forms of human retinal degenerations result from mutations in rhodopsin, arrestin, and phosphodiesterase, among others. Individuals with Oguchi disease have mutations in visual arrestin and a form of degenerative night blindness (*24*). Rescue of degeneration in *Drosophila* visual mutants provides a strong basis for exploring strategies that manipulate sphingolipid enzymes for therapeutic management of retinal degeneration in higher organisms.

References and Notes

1. Y. A. Hannun, C. Luberto, K. M. Argraves, *Biochemistry* **40**, 4893 (2001).
2. S. Spiegel, D. English, S. Milstien, *Trends Cell Biol.* **12**, 236 (2002).
3. M. Nikolova-Karakashian, A. H. Merrill Jr., *Methods Enzymol.* **311**, 194 (2000).
4. K. D'Hondt, A. Heese-Peck, H. Riezman, *Annu. Rev. Genet.* **34**, 255 (2000).
5. D. P. Smith, M. A. Stamnes, C. S. Zuker, *Annu. Rev. Cell Biol.* **7**, 161 (1991).
6. C. Montell, *Annu. Rev. Cell Dev. Biol.* **15**, 231 (1999).
7. J. E. O'Tousa, in *Progress in Retinal Eye Research*, N. N. Osbourne, G. J. Chader, Eds. (Elsevier, New York, 1997), p. 691.
8. P. J. Dolph *et al.*, *Science* **260**, 1910 (1993).
9. W. E. Miller, R. J. Lefkowitz, *Curr. Opin. Cell Biol.* **13**, 139 (2001).
10. A. Kiselev *et al.*, *Neuron* **28**, 139 (2000).
11. P. G. Alloway, L. Howard, P. J. Dolph, *Neuron* **28**, 129 (2000).
12. A. H. Brand, N. Perrimon, *Development* **118**, 401 (1993).
13. M. Freeman, *Cell* **87**, 651 (1996).
14. Materials and methods are available as supporting material on *Science* Online.
15. X. Han, *Anal. Biochem.* **302**, 199 (2002).
16. T. Adachi-Yamada *et al.*, *Mol. Cell Biol.* **19**, 7276 (1999).
17. J. E. Hinshaw, *Annu. Rev. Cell Dev. Biol.* **16**, 483 (2000).
18. S. Sever, H. Damke, S. L. Schmid, *Traffic* **1**, 385 (2000).
19. C. A. Poodry, *Dev. Biol.* **138**, 464 (1990).
20. J. Dubnau, L. Grady, T. Kitamoto, T. Tully, *Nature* **411**, 476 (2001).
21. N. R. Orem, P. J. Dolph, *Vision Res.* **42**, 497 (2002).
22. D. M. Zerr, J. C. Hall, M. Rosbash, K. K. Siwicki, *J. Neurosci.* **10**, 2749 (1990).
23. A. Claing, S. A. Laporte, M. G. Caron, R. J. Lefkowitz, *Prog. Neurobiol.* **66**, 61 (2002).
24. Q. Wang, Q. Chen, K. Zhao, L. Wang, E. I. Traboulsi, *Ophthalmic Genet.* **22**, 133 (2001).

25. We thank C. Zuker, T. Kitamoto, and the *Drosophila* stock center (Bloomington, Indiana) for fly stocks; M. Mowen and K. Stanard for technical assistance; and C. Zuker, V. Malhotra, M. Fortini, I. Daar, and A. Weissman for comments on the manuscript.

Supporting Online Material

www.sciencemag.org/cgi/content/full/299/5613/1740/DC1
Materials and Methods
Figs. S1 and S2

18 November 2002; accepted 3 January 2003

Dissecting Temporal and Spatial Control of Cytokinesis with a Myosin II Inhibitor

Aaron F. Straight,[1]* Amy Cheung,[1] John Limouze,[2] Irene Chen,[3] Nick J. Westwood,[4] James R. Sellers,[2] Timothy J. Mitchison[1]

Completion of cell division during cytokinesis requires temporally and spatially regulated communication from the microtubule cytoskeleton to the actin cytoskeleton and the cell membrane. We identified a specific inhibitor of nonmuscle myosin II, blebbistatin, that inhibited contraction of the cleavage furrow without disrupting mitosis or contractile ring assembly. Using blebbistatin and other drugs, we showed that exit from the cytokinetic phase of the cell cycle depends on ubiquitin-mediated proteolysis. Continuous signals from microtubules are required to maintain the position of the cleavage furrow, and these signals control the localization of myosin II independently of other furrow components.

Cytokinesis is the process by which daughter cells are separated from one another at the end of cell division. During cytokinesis, the cell cycle, cytoskeleton, and membrane systems of the cell undergo a linked, closely coordinated series of changes on a time scale of minutes (*1*, *2*). Two outstanding questions dominate the field of cytokinesis: What timing mechanisms control progress through cytokinesis, and how is the cleavage furrow positioned to divide the cell into two equal parts? The cleavage furrow is positioned on a plane that bisects the axis of chromosome segregation by microtubules associated with the mitotic apparatus (*3*), but the signals used to communicate between the microtubules and the furrow are largely unknown. Pathways that control the timing of progression through cytokinesis to the G_1 phase of the

[1]Department of Cell Biology and Institute of Chemistry and Cell Biology, Harvard Medical School, 250 Longwood Avenue, Boston, MA 02115, USA. [2]Laboratory of Molecular Cardiology, National Heart, Lung, and Blood Institute, National Institutes of Health, Bethesda, MD 20892, USA. [3]Department of Molecular Biology, Massachusetts General Hospital, Boston, MA 02114, USA. [4]School of Chemistry, University of St. Andrews, St. Andrews, Fife, KY16 9AJ, UK.

*To whom correspondence should be addressed. E-mail: aaron_straight@hms.harvard.edu

cell cycle have been identified with genetic studies in yeast (*4*, *5*). Components of these pathways are conserved, but their relevance to mammalian cytokinesis is unclear.

We took a small molecule–based approach to dissect the logic of cytokinesis in mammalian cells. Previous small-molecule work using microtubule or actin depolymerizers (colchicine, nocodazole, or cytochalasin) has demonstrated the importance of microtubules for both positioning (*3*) and ingression (*6*) of the cytokinesis furrow, and of actin for the structure of the furrow (*7*). Actin and microtubule inhibition have also revealed the existence of an ~1-hour window after anaphase during which the cell is competent to undergo cytokinesis, called C phase (*8*, *9*). To investigate further, we wanted a small molecule that would arrest furrow ingression, but not perturb furrow assembly. We therefore targeted nonmuscle myosin II, which provides the force for furrow ingression (*10*, *11*), using a high-throughput screening assay (*12*, *13*). Blebbistatin (Fig. 1A, fig. S1) inhibited both the adenosine triphosphatase (ATPase) and gliding motility activities of human platelet nonmuscle myosin II without inhibiting myosin light chain kinase (fig. S2). We separated the enantiomers (*13*) and found that (–)-blebbistatin is the active species, with an inhibitory concentration for 50% inhibition (IC_{50}) of ~2 μM, whereas (+)-blebbistatin was inactive (Fig. 1A). Rabbit skeletal and human nonmuscle myosin II were inhibited by blebbistatin, but human myosins Ib, Va, and X were not (Fig. 1B).

Blebbistatin blocked myosin II–dependent cell processes. The compound's name is derived from its ability to block cell blebbing rapidly (within ~2 min) and reversibly (fig. S3, movie S1). It also rapidly disrupted directed cell migration (fig. S3, movie S2) and cytokinesis in vertebrate cells (Fig. 1C). Blebbistatin did not affect *Drosophila melanogaster* cells. Inhibition was specific for the (–) isomer, consistent with myosin II being the relevant drug target (Fig. 1D). Addition of blebbistatin to dividing cells blocked furrow ingression within 5 min and was reversible (movies S3 and S4). Blebbistatin did not block assembly of either the furrow or the microtubules that position it. In arrested cells, two major furrow components, myosin II and anillin (*14*, *15*), were localized to an equatorial ring, and microtubules were organized into two prominent cytokinesis-associated arrays: a bipolar midzone complex between the separated chromosomes and asters radiating from the centrosomes to the furrow (Fig. 1E). This organization resembled that seen in control cells, except for the lack of furrow contraction (Fig. 1E). Thus, blebbistatin can be used to probe the spatial organization of the cytokinesis machinery in the absence of furrow contraction.

We examined the timing of mitotic exit in blebbistatin. Staining for DNA and nuclear lamins showed that chromosome decondensation and nuclear envelope reformation occurred in the presence of blebbistatin (Fig. 2A), and time-lapse microscopy demonstrated that the timing of these events was unaffected by the drug (fig. S4) (*13*). Blebbistatin-treated HeLa cells initiated DNA replication ~12 hours after release from mitosis, like untreated cells; HeLa cells lack the checkpoint that prevents entry into S phase if mitosis fails (*16*, *17*). Thus, blocking furrow contraction does not in itself prevent exit from mitosis, although clearly these events must be coordinated in normal cells.

We next investigated the timing of C phase. C-phase initiation is triggered by anaphase onset and requires the anaphase-promoting complex (APC) and ubiquitin-mediated proteolysis (*18*). We measured the duration of C phase in the presence of blebbistatin by allowing cells to initiate anaphase in the presence of blebbistatin, then removing the drug at increasing intervals and monitoring furrowing. Unsynchronized cells remained competent to contract for 45 to 60 min after anaphase onset as determined by time-lapse imaging (*13*). The ~1-hour duration of C phase in the presence of blebbistatin is similar to its reported duration in the presence of an actin-depolymerizing drug (*8*) and the

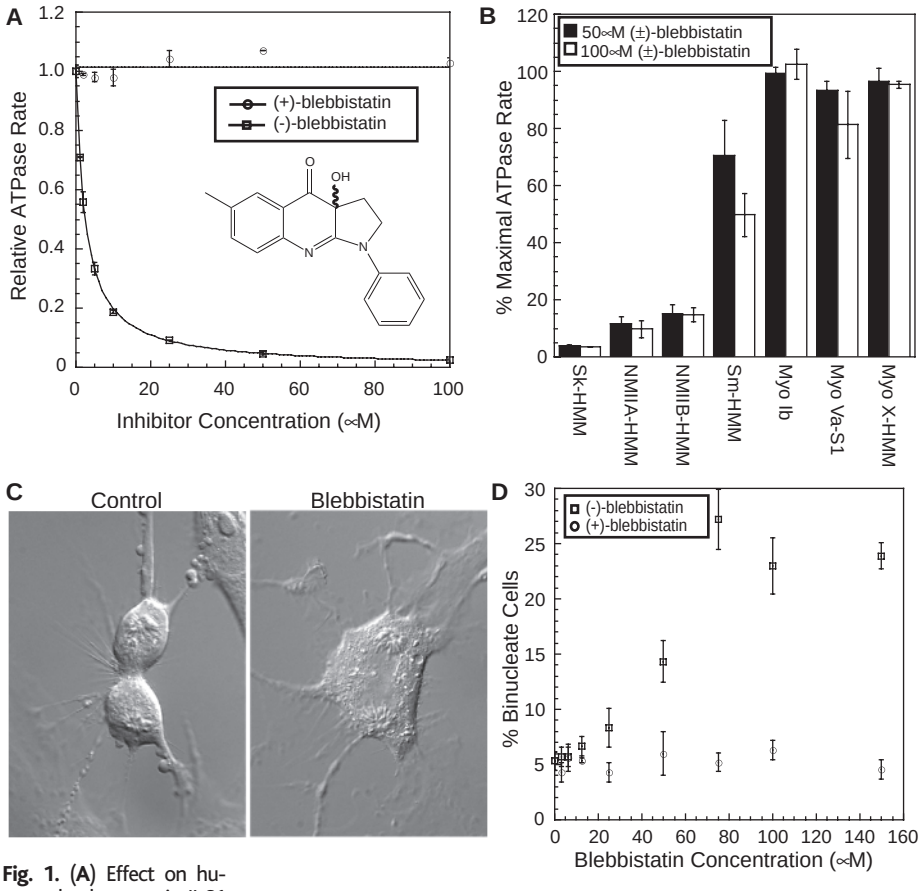

Fig. 1. (**A**) Effect on human platelet myosin II S1 Mg · ATPase by active (–) enantiomer (squares) and inactive (+) enantiomer (circles) of blebbistatin. (Inset) The structure of (±)-blebbistatin. (**B**) Effects of (±)-blebbistatin on the actin-activated ATPase rate of muscle and nonmuscle myosins. Myo X-HMM, myosin *X*-heavy meromyosin; Myo Va-S1, myosin Va-subfragment 1; Myo 1b, myosin 1b; Sm-HMM, smooth muscle myosin II-HMM, NMIIB-HMM, nonmuscle myosin IIB-HMM; NMII-HMM, nonmuscle myosin II-HMM; Sk-HMM, skeletal muscle myosin II-HMM. (**C**) Cytokinetic *Xenopus* tissue culture cells with or without 100 μM (±)-blebbistatin. (**D**) Comparison of (+) (circles) versus (–) (squares) enantiomers of blebbistatin on binucleate cell formation in HeLa cells. (**E**) HeLa cells untreated (control) or treated (blebbistatin) with 100 μM (±)-blebbistatin and stained for DNA (blue), α-tubulin (green), and nonmuscle myosin II (red).

window of cortical contractility after anaphase onset (*9*), suggesting that an unidentified cell-cycle signal terminates C phase. In synchronized cells, C phase was scored by the presence of the microtubule midzone and of an equatorial ring of myosin II and anillin. Synchronized cells acquired these markers beginning ~60 min after release from a mitotic block into blebbistatin (*13*) and lost them over the next 60 to 90 min.

In yeast, APC-dependent proteolysis is required to exit mitosis (*19*, *20*). We therefore tested whether the proteasome inhibitor MG132 (*21*) affected C-phase duration in synchronized HeLa cells released from mitosis into blebbistatin. MG132 was added after >75% of the cells had initiated anaphase, and samples were fixed at different time points. The percentage of binucleate cells that retain a myosin II ring after 135 min is significantly increased by MG132 (Fig. 2B). Because cells that had not initiated anaphase before MG132 addition remained arrested in metaphase by the drug, our data underestimate the effect of MG132. We estimate that MG132 more than doubles the duration of C phase. Cells fixed at 170 min after treatment with both blebbistatin and MG132 mostly retained a midzone complex, although it was often pushed to one side of the cell by the decondensed nuclei (Fig. 2C), and myosin II and anillin remained localized to regions of the cortex closest to the displaced midzone. In contrast, cells treated with blebbistatin alone showed interphase microtubule organization and delocalized myosin II and anillin (Fig. 2C). These data reveal a role for ubiquitin-dependent

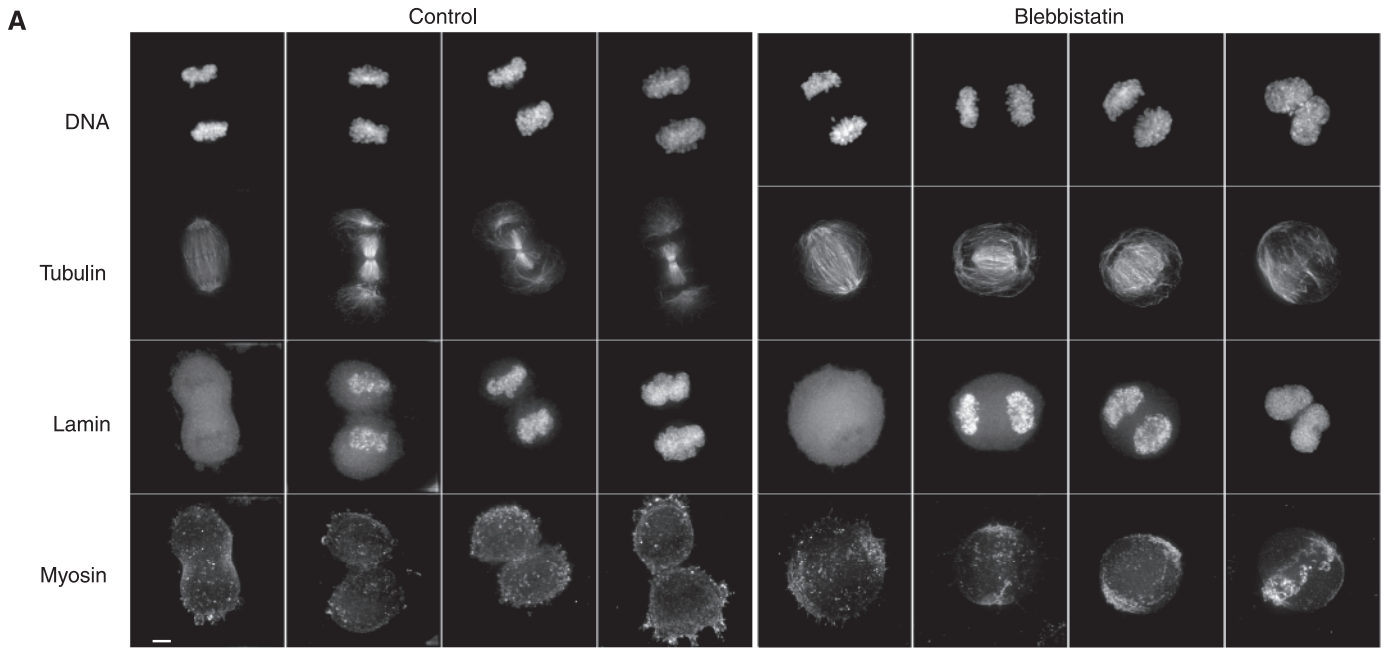

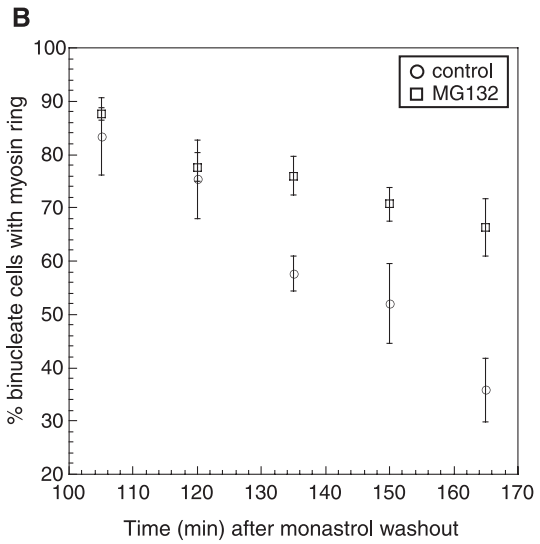

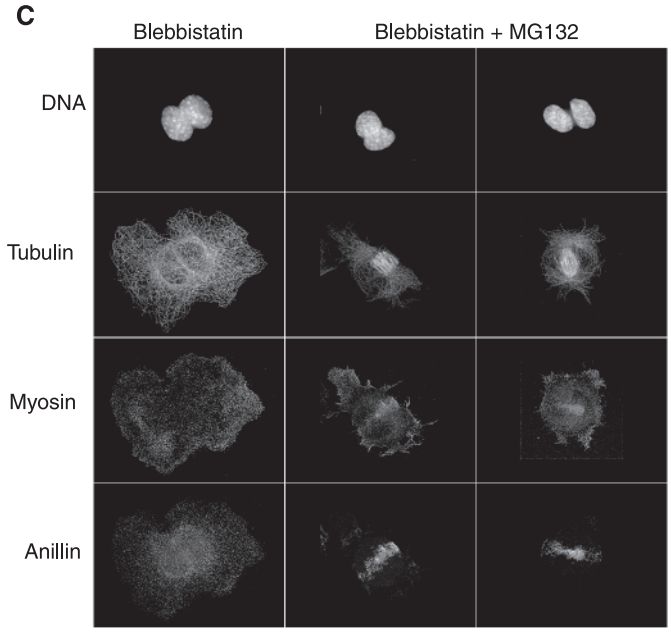

Fig. 2. (**A**) Mitotically synchronized HeLa cells released into medium without (Control) or with (Blebbistatin) 100 μM (±)-blebbistatin. Cells in different stages after anaphase were stained for DNA, α-tubulin, lamins, and nonmuscle myosin II. (**B**) Quantitation of the presence of localized myosin in binucleate cells treated without (circles) or with (squares) MG132 in the presence of blebbistatin ($n = 3$ independent experiments; bars represent standard error). Mitotically synchronized HeLa cells were released into blebbistatin for 80 min then treated without or with 100 μM MG132. Cells were fixed at 15 min intervals after release from mitosis and stained for DNA, α-tubulin, nonmuscle myosin II, and anillin. (**C**) Cells treated as described in (B) and fixed at 170 min after release from metaphase.

proteolysis in C-phase exit in mammalian cells.

To examine how cytokinesis is spatially controlled, we used blebbistatin to probe microtubule-to-cortex communication. Cells arrested in mitosis with the Eg5 kinesin inhibitor monastrol were released into blebbistatin for ~1 hour to allow the initiation of anaphase and furrow assembly. In the continued presence of blebbistatin, we then added other drugs (Fig. 3). Spindle assembly was complete before the new drug was added, and thus we could probe the roles of components required for spindle assembly, such as microtubules. Depolymerizing microtubules by adding nocodazole caused delocalization of both myosin II and anillin. Thus, microtubule-to-cortex communication was required continuously to maintain the localization of furrow components. This is consistent with the observation that microtubules are required for furrow ingression as well as furrow establishment (*6*). Nocodazole treatment also caused the separated nuclei to collapse back together (Fig. 3), suggesting that the midzone is required to keep the nuclei apart until cytokinesis is finished. Actin depolymerization with latrunculin delocalized myosin II and anillin, as expected, and had little effect on the organization of cytokinesis-associated microtubules. In other systems, perturbation of the actin cytoskeleton was reported to cause loss of midzone microtubules (*22*, *23*). We did observe subtle disorganization of microtubules in latrunculin, but overall our data suggest that, in HeLa cells, communication from microtubules to the cortex is primarily unidirectional.

We next investigated the nature of the signals involved. The broad-spectrum kinase inhibitor staurosporine (*24*) caused extensive disorganization, although not complete removal, of midzone microtubules, indicating a role for kinases in midzone organization. Polo and aurora B are candidates for the kinase involved (*25–27*), but staurosporine does not substantially inhibit polo kinase at the concentration used in the experiment (*28*). The effect of staurosporine on aurora B has not yet been determined, so we tested two known ATP competitive inhibitors of aurora B [Compound 1, table 1, of (*29*) and Compound 1, table 1, of (*30*)]. These inhibitors gave results similar to those obtained with staurosporine treatment, causing disruption of the microtubule midzone (fig. S5).

Staurosporine also caused delocalization of myosin II but not of anillin. This provides evidence that localization of anillin and myosin II, which are normally colocalized in the furrow (*31*), are independently controlled. Aurora kinase inhibitors also caused delocalization of myosin II but not of anillin. The

Table 1. Effects of drug treatments on nonmuscle myosin II, anillin, and the microtubule midzone in the presence of (±)-blebbistatin as described for Fig. 3. ER, endoplasmic reticulum.

Target	Drug	Mechanism	Myosin	Anillin	Midzone
Tubulin	Nocodazole	Depolymerization	Delocalized	Delocalized	Absent
	Taxol	Stabilization	No effect	No effect	Robust
Actin	Latrunculin	Depolymerization	Delocalized	Delocalized	Disorganized
Kinases	Staurosporine	General inhibition	Delocalized	No effect	Disrupted
	Aurora-I	Aurora kinase	Delocalized	No effect	Disrupted
	Y27632	Rho-kinase	Delocalized	No effect	No effect
	Olomoucine	CDK	No effect	No effect	No effect
	Alsterpaullone	CDK	No effect	No effect	No effect
	Roscovitine	CDK	No effect	No effect	No effect
Proteolysis	MG132	Proteasome	Prolonged	Prolonged	Prolonged
Kinesins	Monastrol	Eg5 inhibition	No effect	No effect	No effect
Secretion	Brefeldin	ER-Golgi transport	No effect	No effect	No effect

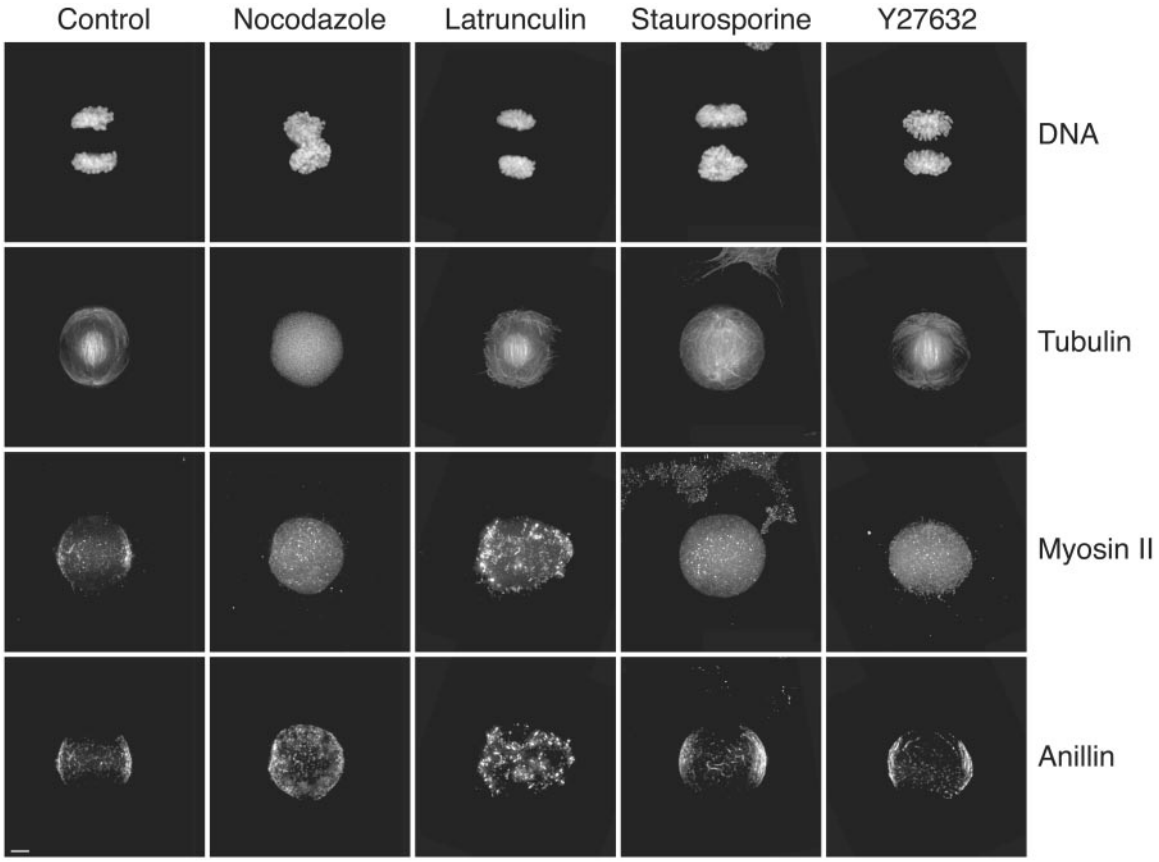

Fig. 3. Effect of inhibitors on the microtubule spindle and the contractile ring in blebbistatin-treated cells. Mitotically synchronized HeLa cells were released into the presence of 100 μM (±)-blebbistatin, then blebbistatin alone (control), nocodazole, latrunculin, staurosporine, or Y27632 was added. Cells were stained for DNA, α-tubulin, nonmuscle myosin II, and anillin.

Rho-kinase inhibitor Y27632 (*32*) had no detectable effect on microtubule organization, delocalized myosin II, and again did not perturb anillin. Thus, Rho-kinase is required to localize myosin II to furrows in blebbistatin-arrested cells, which is broadly consistent with previous data (*33*), and other kinases, probably including aurora B, are required for midzone organization.

Cyclin-dependent kinase (CDK) inhibitors and monastrol do not perturb the cytology of blebbistatin-arrested cells (Table 1). Thus, CDKs do not appear to be directly involved in maintaining the contractile ring after anaphase, although it is possible that they might influence C-phase timing. The target of monastrol, the mitotic kinesin Eg5, is thought to have a central role in the establishment of spindle bipolarity, but our data suggest that it is not responsible for bipolar organization of the midzone during cytokinesis.

Our experiments emphasize the usefulness of fast-acting and reversible drugs in a dynamic cellular pathway such as cytokinesis. It is impossible to determine whether Eg5, for example, is required in cytokinesis with simple ablation experiments, because the ablation of Eg5 disrupts mitosis. New drugs that target guanosine triphosphatases, membrane dynamics, and mitotic motors will be useful in further dissecting the logic of cytokinesis. These proteins and processes are all required for cytokinesis (*1*, *2*), but their precise roles in timing and spatial organization have yet to be defined.

References and Notes

1. A. F. Straight, C. M. Field, *Curr. Biol.* **10**, R760 (2000).
2. M. Glotzer, *Annu. Rev. Cell Dev. Biol.* **17**, 351 (2001).
3. R. Rappaport, *Cytokinesis in Animal Cells* (Developmental and Cell Biology Series 32, Cambridge Univ. Press, Cambridge, UK, 1996).
4. D. McCollum, K. L. Gould, *Trends Cell Biol.* **11**, 89 (2001).
5. A. J. Bardin, A. Amon, *Nature Rev. Mol. Cell Biol.* **2**, 815 (2001).
6. S. P. Wheatley, Y. Wang, *J. Cell Biol.* **135**, 981 (1996).
7. J. R. Peterson, T. J. Mitchison, *Chem. Biol.* **9**, 1 (2002).
8. S. N. Martineau, P. R. Andreassen, R. L. Margolis, *J. Cell Biol.* **131**, 191 (1995).
9. J. C. Canman, D. B. Hoffman, E. D. Salmon, *Curr. Biol.* **10**, 611 (2000).
10. I. Mabuchi, M. Okuno, *J. Cell Biol.* **74**, 251 (1977).
11. A. De Lozanne, J. A. Spudich, *Science* **236**, 1086 (1987).
12. A. Cheung *et al.*, *Nature Cell Biol.* **4**, 83 (2002).
13. Materials and methods are available as supporting material on *Science* Online.
14. K. Fujiwara, T. D. Pollard, *J. Cell Biol.* **71**, 848 (1976).
15. C. M. Field, B. M. Alberts, *J. Cell Biol.* **131**, 165 (1995).
16. A. Hirano, T. Kurimura, *Exp. Cell Res.* **89**, 111 (1974).
17. P. R. Andreassen, O. D. Lohez, F. B. Lacroix, R. L. Margolis, *Mol. Biol. Cell* **12**, 1315 (2001).
18. C. B. Shuster, D. R. Burgess, *Curr. Biol.* **12**, 854 (2002).
19. R. Wasch, F. R. Cross, *Nature* **418**, 556 (2002).
20. J. M. Peters, *Mol. Cell* **9**, 931 (2002).
21. A. F. Kisselev, A. L. Goldberg, *Chem. Biol.* **8**, 739 (2001).
22. M. Gatti, M. G. Giansanti, S. Bonaccorsi, *Microsc. Res. Tech.* **49**, 202 (2000).
23. D. Cimini, D. Fioravanti, C. Tanzarella, F. Degrassi, *Chromosoma* **107**, 479 (1998).
24. U. T. Ruegg, G. M. Burgess, *Trends Pharmacol. Sci.* **10**, 218 (1989).
25. R. M. Golsteyn, K. E. Mundt, A. M. Fry, E. A. Nigg, *J. Cell Biol.* **129**, 1617 (1995).
26. Y. Terada *et al.*, *EMBO J.* **17**, 667 (1998).
27. M. Murata-Hori, Y. L. Wang, *J. Cell Biol.* **159**, 45 (2002).
28. D. Fabbro *et al.*, *Pharmacol. Ther.* **82**, 293 (1999).
29. J. F. Henri, B. A. George, K. N. John, M. A. Austen, World Intellectual Property Organization (WPO) Patent #WO0121596. (2001).
30. J. F. Henri, M. A. Austen, WPO Patent #WO0155116 (2001).
31. K. Oegema, M. S. Savoian, T. J. Mitchison, C. M. Field, *J. Cell Biol.* **150**, 539 (2000).
32. M. Uehata *et al.*, *Nature* **389**, 990 (1997).
33. H. Kosako *et al.*, *Oncogene* **19**, 6059 (2000).

34. We thank E. M. Ostap for purified myosin Ib; J. Dantzig, A. Shaw, and Y. M. Goldman for rabbit skeletal myosin SI; L. Flanagan and T. Stossel for M2 cells; K. Pierce and M. M.-C. Lo for assistance with chiral chromatography; S. Miller and T. Kapoor for advice on chemical synthesis; T. Kapoor for assistance with aurora kinase inhibitors; and A. Farrell, W. Brieher, and R. Ward for stimulating discussion and critical review of the manuscript. This work was supported by grants from the NIH (GM62566, GM23928) to T.J.M. and from Merck & Co. and E. Merck. A.F.S. was supported by the Cancer Research Fund of the Damon Runyon–Walter Winchell Foundation.

Supporting Online Material

www.sciencemag.org/cgi/content/full/299/5613/1743/DC1
Materials and Methods
Figs. S1 to S6
References and Notes
Movies S1 to S4

11 December 2002; accepted 4 February 2003

Protein Insertion into the Mitochondrial Inner Membrane by a Twin-Pore Translocase

Peter Rehling,[1] Kirstin Model,[2] Katrin Brandner,[1,3] Peter Kovermann,[4] Albert Sickmann,[5] Helmut E. Meyer,[5] Werner Kühlbrandt,[2] Richard Wagner,[4] Kaye N. Truscott,[1] Nikolaus Pfanner[1]*

The mitochondrial inner membrane imports numerous proteins that span it multiple times using the membrane potential $\Delta\psi$ as the only external energy source. We purified the protein insertion complex (TIM22 complex), a twin-pore translocase that mediated the insertion of precursor proteins in a three-step process. After the precursor is tethered to the translocase without losing energy from the $\Delta\psi$, two energy-requiring steps were needed. First, $\Delta\psi$ acted on the precursor protein and promoted its docking in the translocase complex. Then, $\Delta\psi$ and an internal signal peptide together induced rapid gating transitions in one pore and closing of the other pore and drove membrane insertion to completion. Thus, protein insertion was driven by the coordinated action of a twin-pore complex in two voltage-dependent steps.

The mitochondrial inner membrane contains two translocases that are responsible for the specific import of hundreds of different proteins (*1–4*). The presequence translocase (TIM23 complex) typically transports hydrophilic preproteins with amino-terminal presequences by using the inner membrane potential $\Delta\psi$ for initiation of translocation and the ATP-driven Hsp70 motor for completion of transport. The protein insertion complex (TIM22 complex, carrier translocase) carries out the insertion of numerous abundant multispanning inner membrane proteins, e.g., metabolite carriers, that contain internal targeting signals. The TIM22 complex of ~300 kD contains six subunits, the integral membrane proteins Tim54, Tim22, and Tim18 and the peripheral proteins Tim12, Tim10, and Tim9 (*1–4*). Its function depends on only one external energy source, the membrane potential $\Delta\psi$. Purified Tim22 forms a single pore that is voltage-activated and responds to a synthetic signal peptide (*5*). How the TIM22 complex inserts membrane proteins that contain multiple transmembrane segments is unclear, because the entire complex has never been purified in a functional form. Also, how $\Delta\psi$ alone can drive the import and insertion of multispanning inner membrane proteins remains unclear.

We developed a strategy to isolate the yeast mitochondrial TIM22 complex. When we tagged Tim18 with ProtA, which contains two immunoglobulin G (IgG)–binding do-

[1]Institut für Biochemie und Molekularbiologie, Universität Freiburg, Hermann-Herder-Strasse 7, D-79104 Freiburg, Germany. [2]Max-Planck Institut für Biophysik, Abteilung Strukturbiologie, Heinrich-Hoffmann-Strasse 7, D-60528 Frankfurt am Main, Germany. [3]Fakultät für Biologie, Universität Freiburg, D-79104 Freiburg, Germany. [4]Biophysik, Universität Osnabrück, FB Biologie/Chemie, D-49034 Osnabrück, Germany. [5]Medizinisches Proteom-Center, Gebäude ZKF E/143, Ruhr-Universität Bochum, Universitätsstrasse 150, D-44780 Bochum, Germany.

*To whom correspondence should be addressed. E-mail: Nikolaus.Pfanner@biochemie.uni-freiburg.de